Numerical Study to Investigate the Pressure Propagation Patterns by a Compression Sleeve with Miniaturised Air-bladders

Dilshan Hedigalla
Dept. of Textile and Apparel Engineering
University of Moratuwa
Katubedda, Sri Lanka.
dilshanpoorna412@gmail.com

Malindu Ehelagasthenna
Dept. of Mechanical Engineering
University of Moratuwa
Katubedda, Sri Lanka.
malindu.ehala@gmail.com

Indrajith D. Nissanka
Dept. of Mechanical Engineering
University of Moratuwa
Katubedda, Sri Lanka.
nissankai@uom.lk

Ranjith Amarasinghe
Dept. of Mechanical Engineering
University of Moratuwa
Katubedda, Sri Lanka.
ranama@uom.lk

Gayani K. Nandasiri
Dept. of Textile and Apparel Engineering
University of Moratuwa
Katubedda, Sri Lanka.
gayanin@uom.lk

***Abstract*—Chronic venous disease(CVD), the most prevalent vascular disease affecting to the lower extremities, is regarded as any functional or morphological abnormalities of the venous system. Compression therapy, either active or passive is currently regarded as the cornerstone of treatment for all CVD related complications. However, most of the existing textile solutions have major limitations of applying uniform pressure around the lower limb circumference which was overcame by applying a radial force in response to the pressure exerted by an air volume trapped inside a miniature bladder. Hence, this article used numerical simulations to investigate the propagation of pressure on the skin, fat and muscle layers applied by hexagonal shaped mini-bladders. The results of this study revealed that 40% of internal pressure of the bladders successfully transmitted through the skin layer, and slight increase of pressure was recorded along the thickness of skin layer while it was decreased in fat and muscle layers. Moreover, the highest percentage of pressure drop was recorded along the muscle layer.**

***Index Terms*—Chronic venous disease, compression therapy, finite element analysis, active compression**

I. Introduction

Chronic venous disease (CVD) including venous ulcers, chronic venous insufficiency (CVI), and varicose veins, is one of the most prevalent chronic medical conditions affecting the lower extremities [1]–[3], [5]; which is regarded as any functional or morphological abnormalities of the venous system [3]–[6].The estimated prevalence of varicose veins is ranging between 10% to 30% of worldwide population and 5% to 30% among adult population in the developed countries [3], [5], [7]. Hence, annually several millions of individuals are seeking treatment for a range of CVD related symptoms: discomfort, leg pain and heaviness, skin discolouration, oedema, lipodermatosclerosis, varicose veins and venous ulceration. Thus, resulting in a global treatment market for the varicose vein to grow form USD 290.59 million in 2016 to USD 396 million in 2021 [8].

Even though, various treatments methods are available for the CVD, compression therapy is currently regarded as the cornerstone of treatment for all CVD related complications [3]–[5], [9]. In compression therapy, an external pressure is applied to the limb resulting in a reduction of the diameter of both deep and superficial veins and increasing the blood flow, thus restoring the functionality of calf pump unit [9]. Compression therapy is currently available in the form of intermittent pneumatic compression (IPC), medical compression stockings (MCS), and medical compression bandages (MCB) all of which can be classified as passive or active compression [3], [5]. In passive compression treatment systems such as MCB and MCS, pressure applied on to the skin is directly proportional to the tangential tension component (T) developed in elastic fabrics due to its stretch [3], [5] and inversely proportional to the radius of the limb (R) [4]. The passive compression devices can exert a graduated pressure from ankle to knee level owing to the effect of radius of curvature and the stretch of the fabric. However, those treatment methods fails to apply an uniform compressive force around the leg circumference due to radius of curvature difference [3]–[5]. Moreover, they lose their elasticity over time, causing to snag, resulting in incorrect pressure profiles [10].

In active compression devices such as single bladder cuffs and multi chamber cuffs, compression force is applied by inflating bladders connected to a pneumatic air pump [3], [11]. Single bladder cuffs are incapable of creating a pressure gradient across the entire limb as it expands and contracts completely [3], while multi chamber cuffs typically consist of three to four chambers provides a sequential compression as it

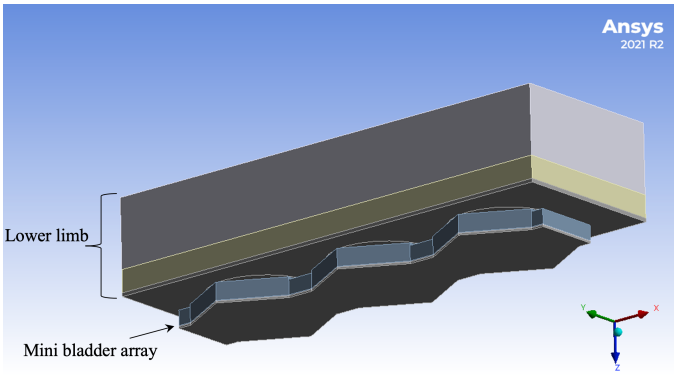

Fig. 1. Solid model of numerical simulation

inflate sequentially from ankle to knee level and then deflate them all at once [3], [11]. However, these pneumatic cuffs are bulkier and uncomfortable to wear due to the large size of the bladders [3], [11]. In recent past, active compression devices based on active materials such as dielectric elastomer actuators (DEAs), shape memory polymers (SMPs), and shape memory alloys (SMAs) have been researched to overcome the drawbacks associated with the MCB, MCS and IPC [12]–[15]. However, these devices exert pressure on the limb based on the tension generated due to the deformation of the active material. Hence, the uniform pressure around the limb's circumference could not be achieved by these methods due to the effect of radius of curvature [12]–[15].

Hence, an active compression device which could apply a radial force in response to the pressure exerted by an air volume trapped inside a miniature bladder was developed to overcome the limitations associated with existing compression devices [3], [5]. Even though it was shown that hexagonal shaped mini bladders [3], [5] arranged in a compression sleeve could effectively apply an uniform pressure on to lower limb, the propagation of pressure on the skin, fat and muscle has not yet been investigated. Moreover, most of the published numerical research studies on estimating the pressure applied by compression garments have considered the lower limb as a homogeneous material and have extended the study of the pressure distribution on the skin layer. This was due to the lack of data availability, variations in thickness, properties of the skin, fat and muscle layers as well as the higher variance exists among humans [16]–[19]. Thus, this numerical analysis aims to investigate the propagation of pressure on to the skin, fat and muscle layers. The outcome of this analysis is expected to be used to deduce the optimum mini-bladder sizes and arrangement towards the development of an active compression sleeve for the treatment of CVD.

II. Methodology

In this study, numerical simulations were used in determining the propagation of the pressure towards skin, fat and muscle layers. The simulation model was developed in ANSYS 2021® and simulations were conducted on a cuboidal shaped section. Even though the lower limb has a curved surface, the selection of the cuboidal shape will not significantly affect the results, as the pressure applied by the mini-bladder around the limb circumference has proven to be uniform [3], [5]. This numerical approach of the study aims to analyze the pressure propagation through the soft tissues as the mini hexagonal shaped mini bladders could exert an uniform pressure around the circumference.

A. Geometric model

A cuboid shaped section including skin, fat and muscle tissue layers shown in Fig.1, was designed using SOLIDWORKS 2020®.The developed solid model was used to study the pressure transmission characteristics of hexagonal shaped mini-bladders with external side length 20mm. Thickness of the each tissue layer shown in Table I, was chosen based on the previous literature [20]–[22]. Inflatable mini-bladder array was designed with three hexagonal shaped mini bladders having external side length of 20mm, similar to the previous study [3], [5], which is shown in Figure 1. The mini-bladders were designed such that only one surface of the mini bladder that is in contact with the skin could be inflated while inflation of all the other surfaces were restricted to increase the efficiency of pressure transmission of mini bladders. The mini-bladders were developed with three layers: top elastomer layer including inflatable chambers in which hexagonal surfaces directly contact with the skin and fully inflates to exert desired level of pressure, a fabric layer, and another bottom elastromer layer. The fabric based bottom layer was utilized as the base layer instead of rigid material to reduce the rigidity of the compression device while it restricts the inflation of the bottom layer. The gap distance between the skin surface and the hexagonal shaped top layers was set as 2mm.

B. Material models and Meshing

Skin, fat and muscle tissue layers were modeled using Ogden first order model [23] whose selected material parameters were listed in the Table II. Top layer and the bottom layer of the mini-bladders were assumed as a hyper-elastic material with nearly incompressible and was modeled

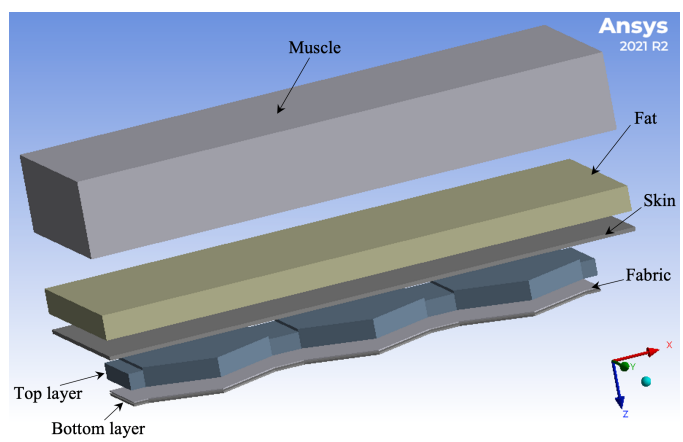

Fig. 2. Solid model of numerical simulation

TABLE I
THICKNESS OF TISSUE LAYERS

Tissue layer	*Site*	*Thickness(mm)*	*Reference*
Skin	Crus	1.32	[20]
Fat	Calf	8.34	[21]
Muscle	Calf	25.8	[22]

TABLE II
MATERIAL PARAMETERS FOR SOFT TISSUES IN REFERENCE MODEL [23]

Soft tissue	μ(MPa)	α(-)
Skin	0.008	10
Fat	0.01	5
Muscle	0.003	30

using Yeoh second order model [3], [5] while fabric layer was modeled as a linear elastic isotropic material [3], [5]. The mesh of all the geometries are generated by first order tetrahedron solid elements. A mesh sensitivity analysis was conducted to determine an acceptable mesh element size for all the geometries, and based on the analysis maximum grid element size of 1mm was selected for the simulations.

C. Boundary and loading conditions

Contacts between all the tissue layers such as skin, fat and muscle, as shown in Fig. 2, were set as bonded [24] while contact between the skin surface and hexagonal surfaces of the top layer was set as frictional with 0.6 frictional coefficient [25]. Moreover, contacts between top, fabric and bottom layers, as shown in Fig. 2, were defined as bonded. All exterior surfaces of skin, fat and muscle tissue layers except interface surfaces and the skin surface, were set as fixed for all rotations and translations. Static pressure was applied to all the internal surfaces of air chamber of the mini-bladders.

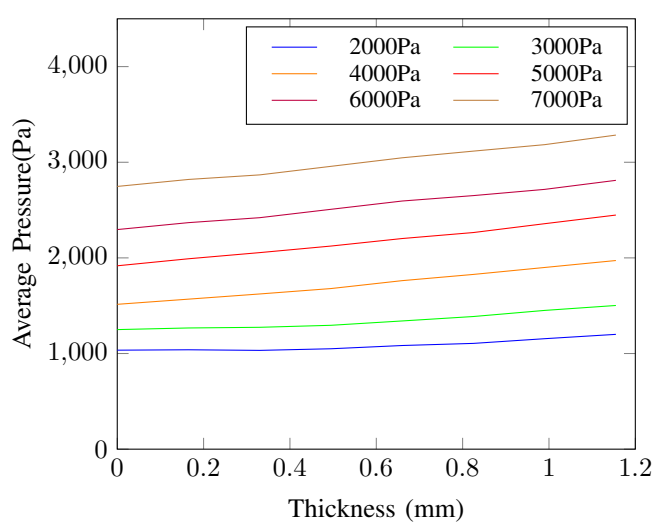

Fig. 3. Pressure transmission in the skin layer

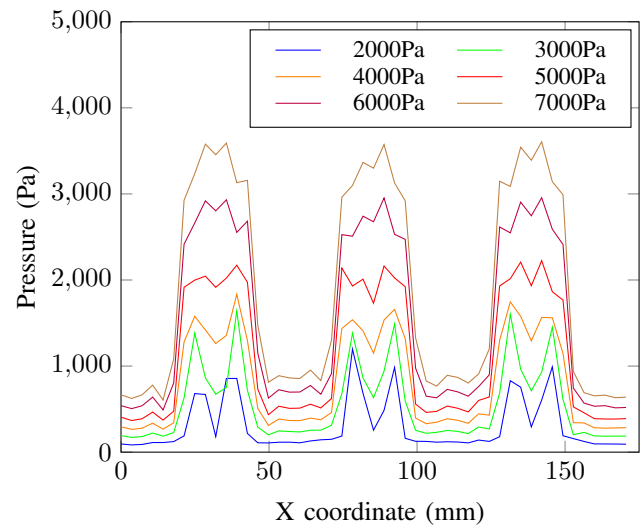

Fig. 4. Pressure transmission inside the skin layer in the longitudinal direction

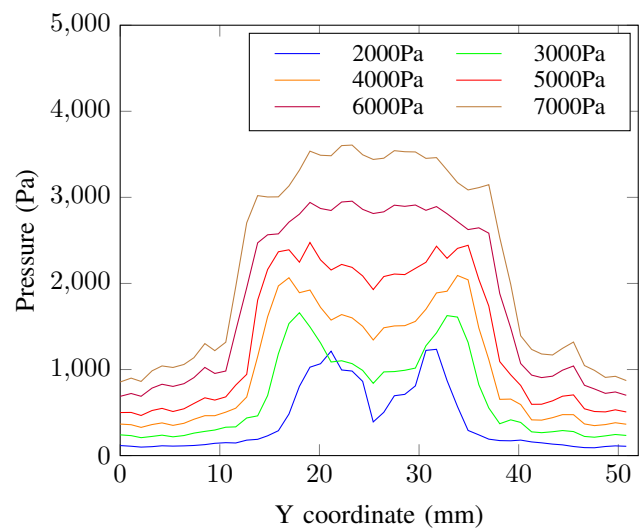

Fig. 5. Pressure transmission inside the skin layer in the transverse direction

D. Data Analysis

Eight planes on each soft tissue layer were defined and the von mises stresses of each plane were calculated when applied pressure varied from 2kPa to 7kPa. The pressure range was selected based on the required pressure profiles for the compression therapy for CVD (i.e. 15 mmHg to 50 mmHg). The results were used to calculate the average pressure on each plane. Moreover, to reconfirm whether the mini-bladders are capable of applying an uniform pressure on to the skin surface as mentioned in the literature [3], [5],the pressure propagation along lengthwise and widthwise directions were also analysed.

III. RESULTS AND DISCUSSION

Since the material properties of individual layers: skin, fat, muscle are different, the corresponding numerical simulation results are discussed accordingly in the subsequent sections.

A. Pressure distribution on the skin layer

Fig. 3 demonstrates the average pressure transmission through the skin layer compressed by air cells at varied applied pressures ranging from 2kPa to 7kPa. There is a slight increase of the pressure throughout the thickness of the skin. The highest pressure was observed at the end of the skin layer (contact surface of skin-fat) for all applied pressures. However, the recorded pressures were always less than the respective applied pressure to the mini-bladders. The percentage transmission of the applied pressure to the skin decreased from 52 % to a plateau of 38-39 % with the increase of the applied pressure. Therefore, these results conclude that the percentage pressure transmission is limited to ≈ 40 % after the applied pressure is more than 3kPa. Consequently, the gap between pressure lines increased with the applied pressure, implying that the rate of increase of pressure transfer increases with the applied pressure. The reason could be explained due to the excess pressure deforming non contact surfaces of the silicone air cells other than deforming the skin.

The Fig. 4, illustrates the propagated pressure inside the skin layer due to the three contacted mini-bladders. Each line of the Fig. 4 represents the applied pressure from 2kPa to 7kPa similar to the Fig. 3. Here, a decline of pressure in the middle region of the mini-bladders is visible in low applied pressures such as 2kPa, 3kPa and 4kPa. Therefore, more uniform propagated pressure due to contacts could be achieved for higher applied pressures compared to lower pressures. A similar variation could also be observed in the transverse direction as shown in Fig. 5. Furthermore, the effective radius where a uniform pressure is propagated could be identified around 10mm- 15mm which accounts for 50-75% of the mini-bladder surface. These results would be useful towards designing of the optimum size and the gap between the air bladders.

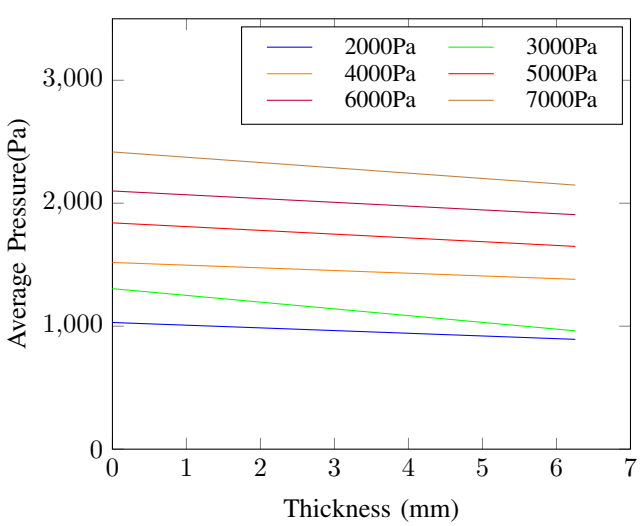

Fig. 6. Pressure transmission in the fat layer

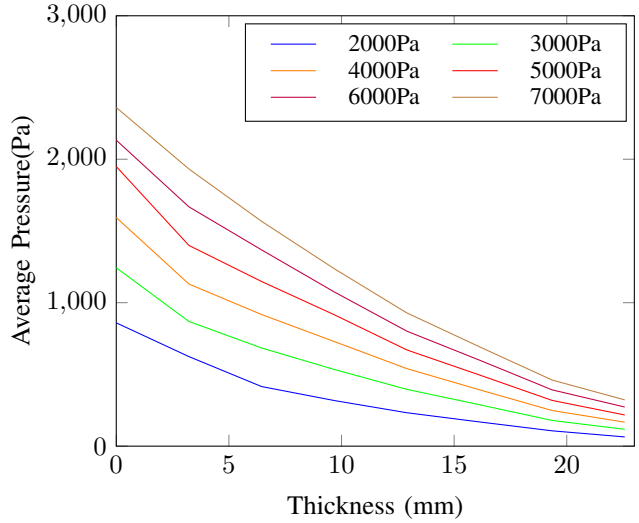

Fig. 7. Pressure transmission in the muscle layer

B. Pressure distribution on the fat layer

Fig. 6 illustrates the pressure transmission through the fat layer for the same applied pressures from 2kPa to 7kPa. The pressure transmission in the fat layer differs from the skin layer for the same applied pressures as the transmitted pressure decreases throughout the thickness of the fat layer. Therefore, the pressure transmission has further reduced after the skin, resulting in further lower pressures propagated in the fat layer.

C. Pressure distribution on the muscle layer

Pressure transmission through the muscle layer when the applied pressure varied from 2kPa to 7kPa is shown in the Fig. 7. As per the Fig. 7 it is clear that the percentage of pressure transmission along the thickness of the muscle layer have decreased for all the applied pressures. However, higher rate of percentage decrease (around 20%) was recorded from 0mm to 6.45mm of the thickness of the muscle layer when applied pressure varied from 1kPa to 5kPa. It was reduced around 10% when the applied pressure varied from 6kPa to 7kPa.Furthermore, when the applied pressure was increased the pressure transmission percentage was also increased, similar to the trends observed in skin and fat layers. However, the percentage of the pressure transmission was higher when the applied pressure increased up to 3kPa and then it gradually decreased for other applied pressures.

Conclusions

This paper presents a numerical study of the pressure propagation on the skin, fat and muscle layers via a compression sleeve comprising of a miniaturised air-bladders. For an effective treatment of CVD it requires a compression of 15-50 mmHg pressure level to facilitate the venous blood return. However, due to the layer of the skin, fat and muscle the applied pressure is mostly not felt by the deep veins which hinders the effectiveness of the compression treatment. This study has extended the studies of miniaturised air-bladders

for the treatment of CVD, where the the pressure propagation profile across the skin layer to the muscle layers (where the deep veins are located) were studied to evaluate the optimum pressure to be delivered to the device.

The results of this study revealed that 40% of internal pressure of the bladders have successfully transmitted through the skin layer, and slight increase of pressure was recorded along the thickness of skin layer while it was decreased in fat and muscle layers. Moreover, the highest percentage of pressure drop was recorded along the muscle layer compared to the skin and the fat layer. Further, when the applied pressure increased, the more uniform pressure propagation was recorded in both longitudinal and transverse directions. Furthermore, the effective radius for propagated uniform pressure could be established as 10mm- 15mm (i.e. 50-75% of the total mini-bladder area). Therefore it can be concluded that the compression sleeve designed with the miniaturised air-bladders should be supplied with more than 250% of the required optimum pressure for the treatment due to propagated pressure loss through the skin, fat and muscle layers. The laboratory experiments are currently ongoing to further validate the results of this numerical study.

Acknowledgment

Authors would like to thank Senate Research Council, University of Moratuwa for the grant SRC/LT/2020/10. Authors wish to acknowledge the Department of Textile and Apparel Engineering and the Department of Mechanical Engineering, University of Moratuwa, Sri Lanka for providing facilities to conduct the research.

References

[1] R. Liu, X. Guo, T. T. Lao, and T. Little, "A critical review on compression textiles for compression therapy: Textile-based compression interventions for chronic venous insufficiency," Text. Res. J., vol. 87, no. 9, pp. 1121–1141, 2017, doi: 10.1177/0040517516646041.

[2] J. L. Beebe-Dimmer, J. R. Pfeifer, J. S. Engle, and D. Schottenfeld, "The epidemiology of chronic venous insufficiency and varicose veins," Ann. Epidemiol., vol. 15, no. 3, pp. 175–184, 2005, doi: 10.1016/j.annepidem.2004.05.015.

[3] G. K. Nandasiri, "A study of use of mini-bladders in active compression as a treatment for venous disease and lymphoedema," no. July, 2019.

[4] J. A. J. Al Khaburi, "Pressure mapping of medical compression bandages used for venous leg ulcer treatment," pp. 5–55, 2010, [Online]. Available: http://etheses.whiterose.ac.uk/3386/1/Thesis_Corrected.pdf.

[5] G. K. Nandasiri, A. Ianakiev, and T. Dias, "Hyperelastic properties of platinum cured silicones and its applications in active compression," Polymers (Basel)., vol. 12, no. 1, pp. 19–23, 2020, doi: 10.3390/polym12010148.

[6] R. D. Langer, E. Ho, and J. O. Denenberg, "Relationships Between Symptoms and Venous Disease: The San Diego Population Study," ACC Curr. J. Rev., vol. 14, no. 10, p. 14, 2005, doi: 10.1016/j.accreview.2005.09.035.

[7] M. Yun et al., "A Study on Prevalence and Risk Factors for Varicose Veins in Nurses at a University Hospital," vol. 9, pp. 4–8, 2018, doi: 10.1016/j.shaw.2017.08.005.

[8] A. H. Davies, "The Seriousness of Chronic Venous Disease: A Review of Real-World Evidence," Adv. Ther., vol. 36, pp. 5–12, 2019, doi: 10.1007/s12325-019-0881-7.

[9] B. Sarı and N. Oğlakcıoğlu, "Analysis of the parameters affecting pressure characteristics of medical stockings," J. Ind. Text., vol. 47, no. 6, pp. 1083–1096, 2018, doi: 10.1177/1528083716662587.

[10] S. T. Yang et al., "An active compression sleeve with variable pressure levels using a wire-fabric mechanism and a soft sensor," Smart Mater. Struct., vol. 28, no. 11, 2019, doi: 10.1088/1361-665X/ab3f56.

[11] R. J. Morris, "Intermittent pneumatic compression - Systems and applications," J. Med. Eng. Technol., vol. 32, no. 3, pp. 179–188, 2008, doi: 10.1080/03091900601015147.

[12] C. Gonçalves, A. F. da Silva, R. Simoes, J. Gomes, L. Stirling, and B. Holschuh, "Design and characterization of an active compression garment for the upper extremity," IEEE/ASME Trans. Mechatronics, vol. 24, no. 4, pp. 1464–1472, 2019, doi: 10.1109/TMECH.2019.2916221.

[13] H. Edher, L. Maupas, S. Nijjer, and A. Salehian, "Utilizing tension reduction in a dielectric elastomer actuator to produce compression for physiological application," J. Intell. Mater. Syst. Struct., vol. 29, no. 5, pp. 998–1011, 2018, doi: 10.1177/1045389X17754254.

[14] B. Kumar, J. Hu, and N. Pan, "Smart medical stocking using memory polymer for chronic venous disorders," Biomaterials, vol. 75, pp. 174–181, 2016, doi: 10.1016/j.biomaterials.2015.10.032.

[15] B. Holschuh and D. Newman, "Two-spring model for active compression textiles with integrated NiTi coil actuators," Smart Mater. Struct., vol. 24, no. 3, p. 35011, 2015, doi: 10.1088/0964-1726/24/3/035011.

[16] R. Liu, Y. Kwok, and Y. Li, "A Three-dimensional Biomechanical Model for Numerical Simulation of Dynamic Pressure Functional Performances of Graduated Compression Stocking (GCS)," vol. 7, no. 4, pp. 389–397, 2006.

[17] E. Ghorbani, H. Hasani, R. J. Nedoushan, and N. Jamshidi, "Finite Element Modeling of the Compression Garments Structural Effect on the Pressure Applied to Leg," vol. 21, no. 3, pp. 636–645, 2020, doi: 10.1007/s12221-020-9542-3.

[18] F. Chassagne, J. Molimard, R. Convert, P. Giraux, and P. Badel, "Numerical Approach for the Assessment of Pressure HAL Id: hal-01380275," no. March, 2016, doi: 10.1007/s10439-016-1597-3.

[19] C. Ye, R. Liu, X. Wu, F. Liang, M. T. C. Ying, and J. Lv, "New analytical model and 3D finite element simulation for improved pressure prediction of elastic compression stockings," Mater. Des., vol. 217, p. 110634, 2022, doi: 10.1016/j.matdes.2022.110634.

[20] L. O. Olsen, H. Takiwaki, and J. Serup, "of of 22," Ski. Res. Technol., no. 294, pp. 74–80, 1995.

[21] Y. Ishida, H. Kanehisa, J. F. Carroll, M. L. Pollock, J. E. Graves, and L. Ganzarella, "Distribution of Subcutaneous Fat and Muscle Thicknesses in Young and Middle-Aged Women," Am. J. Hum. Biol., vol. 9, no. 2, pp. 247–255, 1997, doi: 10.1002/(SICI)1520-6300(1997)9:2¡247::AID-AJHB11¿3.0.CO;2-M.

[22] Y. Huang, J. Zhao, W. Sun, H. Yang, and Y. Liu, "Investigation and modeling of multi-node body channel wireless power transfer," Sensors (Switzerland), vol. 20, no. 1, pp. 1–18, 2020, doi: 10.3390/s20010156.

[23] C. W. J. Oomens, O. F. J. T. Bressers, E. M. H. Bosboom, C. V. C. Bouten, and D. L. Bader, "Can loaded interface characteristics influence strain distributions in muscle adjacent to bony prominences?," Comput. Methods Biomech. Biomed. Engin., vol. 6, no. 3, pp. 171–180, 2003, doi: 10.1080/1025584031000121034.

[24] L. Peko Cohen and A. Gefen, "Deep tissue loads in the seated buttocks on an off-loading wheelchair cushion versus air-cell-based and foam cushions: finite element studies," Int. Wound J., vol. 14, no. 6, pp. 1327–1334, 2017, doi: 10.1111/iwj.12807.

[25] M. Zhang and A. F. T. Mak, "In vivo friction properties of human skin," Prosthet. Orthot. Int., vol. 23, no. 2, pp. 135–141, 1999, doi: 10.3109/03093649909071625.